CONF-820810--19

CONF-820810--19

DE83 009037

THERMAL-HYDRAULIC POSTTEST ANALYSIS FOR THE ANL/MCTF 360° MODEL HEAT-EXCHANGER WATER TEST UNDER MIXED CONVECTION

C. I. Yang, W. T. Sha, and K. E. Kasza

Argonne National Laboratory
Components Technology Division
Argonne, Illinois

As a result of the uncertainties in the understanding of the influence of thermal-buoyancy effects on the flow and heat transfer in Liquid Metal Fast Breeder Reactor heat exchangers and steam generators under off-normal operating conditions, an extensive experimental program is being conducted at Argonne National Laboratory to eliminate these uncertainties. Concurrently, a parallel analytical effort is also being pursued to develop a three-dimensional transient computer code (COMMIX-IHX) to study and predict heat exchanger performance under mixed, forced, and free convection conditions. This paper presents computational results from a heat exchanger simulation and compares them with the results from a test case exhibiting strong thermal buoyancy effects. Favorable agreement between experiment and code prediction is obtained.

1. Introduction

Liquid Metal Fast Breeder Reactor (LMFBR) sodium-to-sodium intermediate heat exchangers (IHXs) under full-flow steady-state normal design operating conditions are not to any measurable degree influenced by thermal buoyancy. However, there are heat-exchanger system interactions which occur during various reactor operation modes for which buoyancy can possibly influence the IHX thermal-hydraulic and structural performance.[1]

There are several areas in which unanswered questions have been raised relative to the importance of thermal buoyancy to IHX performance. First, utilizing high-flow steady-state design conditions, one of the objectives of shell-side inlet-plenum flow-control orificing and tube-bundle/baffle design is to minimize radial tube-bundle temperature variation in order to minimize differential tube expansion and possible buckling problems. However, under low-flow conditions, the shell-inlet plenum and tube-bundle flow paths may be altered by thermal-buoyancy forces, and hence, the tube-bundle thermal field can be changed from the "as designed" thermal distribution. The propensity for the preceding to occur in the IHX, and in steam generators, under various operating conditions has not been adequately studied and evaluated.

Second, the thermal-hydraulic behavior of the LMFBR system under various types of plant transients (i.e., reactor scrams, flow coastdown to natural circulation, evaporator dumps, N-1 loop operation, etc.) is studied using one-dimensional (1-D) flow and energy transport models of the system components. Many of the transient events studied involve the passing from a "high" to a "low" flow with an accompanying rise and/or fall in temperature of the fluid passing through the components. The thermal transients in conjunction with the "low" flow create conditions conducive to thermal-buoyancy effects. The system codes, in addition to using the 1-D assumption, also assume that the classical (neglecting buoyancy) friction and heat-transfer coefficients can be used. Thermal buoyancy can exert its influence on system dynamic-energy transport predictions through alteration of flow and thermal distributions which in turn can influence decay heat removal, system-response time constants, heat transport between primary and secondary loops (via IHX), and thermal-energy rejection at the reactor heat sink (the steam generators). The influence of thermal buoyancy on the above system considerations has not been investigated in great detail and can only be accomplished after the influence of thermal buoyancy on the individual components of the system is understood.

Fluid-flow problems in heat-exchanger units are further complicated by the complex nature of their structural geometry and their heat-transfer processes. The task of detailed analytical analysis is formidable. On the other hand, a simplified approach either analytical or numerical may, under certain circumstances, produce a grossly incorrect solution. Occasions frequently arise when a general, unabridged, three-dimensional transient code becomes desirable. Based on the above, an effort to develop and to validate the COMMIX-IHX[2] code has been initiated.

Under certain favorable flow conditions, vorticity may be created in a thermally nonhomogeneous fluid in motion. It may appear in the form of buoyant vortex rings. For IHX in low-flow thermal-transient tests conducted at ANL/MCTF,[3] such vortex rings or "secondary flow patterns" associated with channeling have been observed in heat exchangers. In a duplicate simulation run with the COMMIX-IHX code such an interesting phenomenon in addition to other transient buoyancy effects have been observed. Comparisons and conclusions regarding

EAB

the numerical and experimental results are presented in the following sections.

2. Test-Article

The heat-exchanger test article, tested in the Argonne National Laboratory Mixing Components Test Facility (MCTF), is a 360°, one-fifth-scale, all-glass, vertically oriented model of a counterflow, single-pass, shell-tube unit. The characteristic features of the test model are shown in Fig. 1.

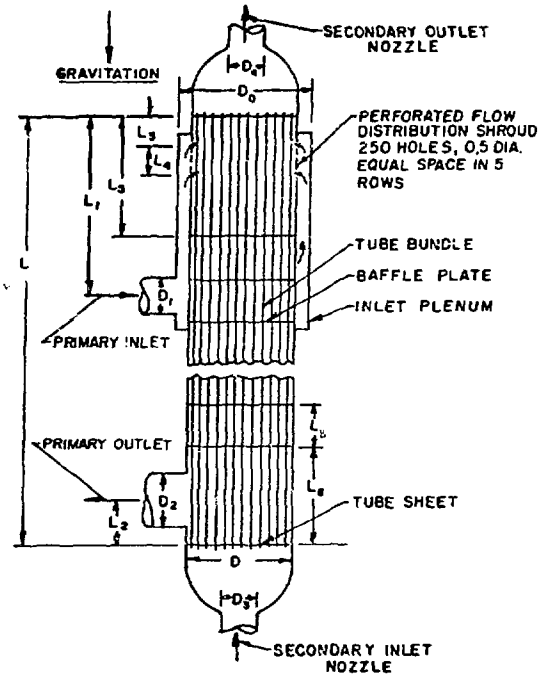

Fig. 1 Geometrical Description of the Test Article.

The relevant dimensions are: L = 200 cm, L_1 = 46 cm, L_2 = 23 cm, L_C = 43 cm, and L_B = 13 cm. These features include: (i) shell inlet plenum, (ii) straight tube bundles (iii) flow-control baffles, and (iv) tube inlet and outlet plenum. To create and promote mixed axial/crossflow in the tube bundle, two types of control baffles, denoted as Types A and B, are used.[3] Ten baffles of Type A and B are located alternately over the tube bundle length. The baffles of Type A are sequentially named as A1, A2, A3, A4, and A5, as are the baffles of Type B. All baffles are of full-disc orificed type. Type A has a 24% perforation in the surrounding annular region and a 60% perforation in the central region. Type B has a 24% perforation in the central region and a 60% perforation in the surrounding annular region.

The uneven distribution of perforations in the baffles is intended for generating and promoting crossflow, hence, to reduce the radial thermal gradient in the HX and to prevent thermal stresses due to the differential expansion between the tubes and the shell.

The shell-side hot-fluid (or cooling flow) enters the inlet plenum through the inlet pipe. It flows upward and through the flow-distribution shroud into the bundle, after passing through the central span of the tube bundle, it then flows out through the lower nozzle to the suction leg of the test facility.

The tube-side cold-fluid (or heating flow) enters the lower inlet plenum, flows upward through 151 straight tubes, and then flows out of the unit through the outlet plenum. Thermocouples were installed at various locations within the test unit, see Fig. 2 for location.

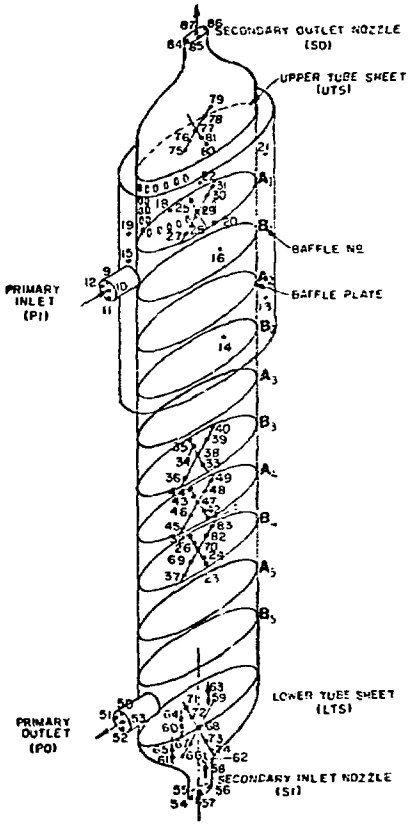

Fig. 2 Heat-Exchanger Baffle Thermocouple Location.

3. Test-Case Description

The test case compared with the COMMIX-IHX numerical prediction in this paper is identified as TX1410. Throughout the entire testing duration, the flow rates at both the shell- and tube-side inlet were kept at constant values of

3.2 m^3/hr. A thermal-transient downramp was then superimposed on the shell-side inlet flow; its temperature drops from 80°C to 40°C in 10 s. while the inlet temperature at the tube-side remained unchanged at 40°C. The thermal transient causes cooler fluid to reside over warmer for a period of time. This situation is unstable and if the buoyancy forces are large enough a strong thermal buoyancy effect can occur, as was the case for this test run.

4. Thermal-Buoyancy Effect in IHX during Thermal-Downramp Transient

Both fluid-flow and heat-transfer behavior profoundly affect the overall performance of the unit. The interactions between the fluid flow and heat transfer along with the complicated geometry present a rather difficult problem for the designer. In general, the flow can be defined and represented by three independent nondimensional parameters. These are Reynolds number, $Re = \frac{UL}{\nu}$, Peclet number, $Pe = \frac{UL}{\alpha}$, and Richardson number $Ri = \frac{g\beta\Delta TL}{U^2}$. U is the characteristic velocity, L is the characteristic length of heat-exchanger; ν, α, and β are kinematic viscosity, diffusivity, and thermal-expansion coefficient of the fluid; ΔT is the reference temperature differential; and g is gravity. The first two parameters can be interpreted as a measure of the relative importance of advective and conductive flux of momentum and heat, respectively. The third parameter is an indicator of the relative importance of the buoyancy force to the inertia force. These three independent parameters can be used to characterize overal thermal-hydraulic behavior of the IHX.

Depending on the importance of the buoyancy force relative to the other forces such as inertia and viscous force, a wide range of dynamical behavior is to be expected. Free convection and forced convection are two extreme cases which have been studied extensively. The intermediate case is known as mixed convection. In the cases of free and mixed convection (test case TX1410, currently under analysis, falls into the mixed-convection category), the buoyancy force is equally or more dominating relative to either inertia or viscous force. For this situation, the velocity and thermal fields are strongly coupled. There is no possibility of determining one independent of the other as could be done in forced convection. For this reason, free and mixed convection is hard to treat, and much of the information about it relies upon experimental investigation and numerical calculations.

In the numerical calculations, the effort to obtain a correct temperature and flow pattern in the shell-side of the heat-exchanger is further complicated by the heat sink created by the heat transfer between the shell- and tube-sides. This is an unique feature of the thermal-hydraulic analysis of the heat-exchanger.

Vorticity not only can be created through viscosity, such as in the boundary layer, but it can also be created through stratification. Vorticity ζ is defined as the curl of velocity. Its governing equation results from taking the curl of the Navier-Stokes equation is,

$$\frac{D\zeta}{Dt} = \zeta \cdot \nabla u + \nu\nabla^2\zeta + \nabla p \times \nabla\left(\frac{1}{\rho}\right). \qquad (1)$$

The term on the left represents the rate of change of vorticity. The first term on the right is the rate of change of vorticity due to stretching and turning of the vortice lines. The second term represest the viscous effect on the diffusion of the vorticity. The last term represents the creation of vorticity due to density variation. This implies that vorticity will be created whenever a nonhomogeneous fluid is displaced from a state in which ∇p and $\nabla\rho$ are parallel. When the body force effectively depends on gravity alone, displacements of density surface away from the horizontal will produce vorticity.

Eq. (1) may explain why certain flow patterns occur in test case TX1410 described previously. The application of the thermal-downramp transient is physically equivalent to the release of a continuous string of negatively buoyant fluid into a relatively warmer surrounding. The temperature differential causes an unstable density gradient. It couples with a pressure gradient and produces a buoyancy force. Such a force provides the source of energy for vortex motion as Eq. (1) suggests. The evolution of the flow pattern changes, resulting from buoyancy forces, is drastic during the transient. When the transient effect starts to diminish, the density gradient $\nabla\rho$ may vanish through convective mixing and the viscous-diffusion process. The vortices will reduce in size and strength. Such vortices have been observed in the present experimental and numerical calculations.

5. Modeling of the Test Article

The test article is partitioned into a number of computational cells using a cylindrical-coordinate system. The primary consideration in partitioning is to limit the number of computational cells to a minimum yet be sufficient to provide the flow and temperature distribution pattern in a desirable resolution. The IHX is partitioned into (6x7x41) computational cells in (θ,r,z) space. Shell inlet and outlet lie in the θ plane bisecting sectors 1 and 4. With the concept of volume porosity and surface permeability, the effects of the tube bundle and baffle plates on

the shell-side flow pattern are accounted for. The flow resistance of the baffles is computed based on empirical correlation. The COMMIX-IHX code did not model the shell inlet plenum of the test model. It was assumed that the flow entered uniformly into the tube bundle through the flow distribution shroud (see Fig. 1).

6. Numerical Results and Discussion

The numerical solution for the steady-state initial conditions of TX1410 were obtained first. The calculated flow patterns are shown in Fig. 3. The computed and measured temperature along the tube bundle central axis near baffles A1, B3, A4, and B4, and near the outlet are shown in Fig. 4.

As shown in Fig. 5, when the thermal-downramp transient occurs, the responses of flow field and temperature distribution are instantaneous and drastic. When the cooler and denser fluid enters the heat-exchanger through the perforated flow-distribution shroud at the top, it creates unstable stratification. Due to density gradient, strong buoyancy forces set the fluid into motion and create vortex rings.

For all the numerical data presented, t=0 is the reference time when the thermal disturbance is passing through the perforated flow-distribution shroud. In the experiment, the reference time t=0 is set when the thermal disturbance is passing through the primary inlet pipe. The difference in the time frame between experiment and code prediction is 24 s. During the

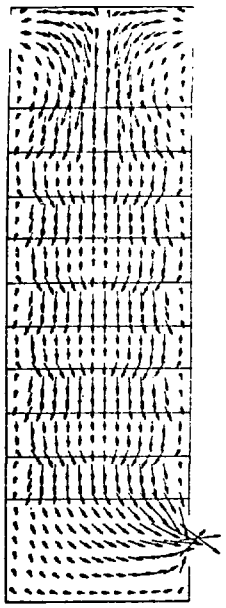

Fig. 3 Flow Pattern at Steady-State Condition.

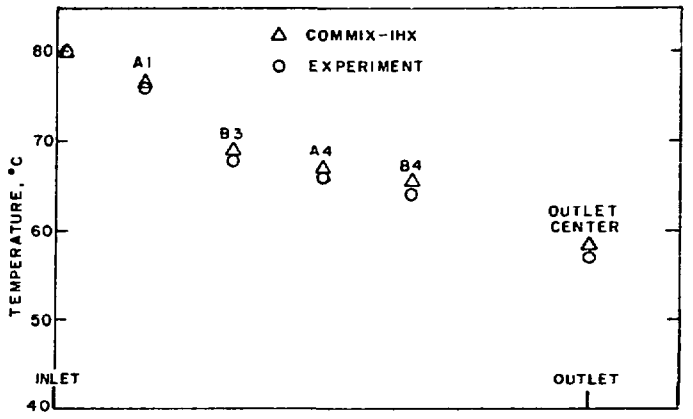

Fig. 4 Comparison of Temperature in Heat-Exchanger for COMMIX-IHX Calculation and Experiment.

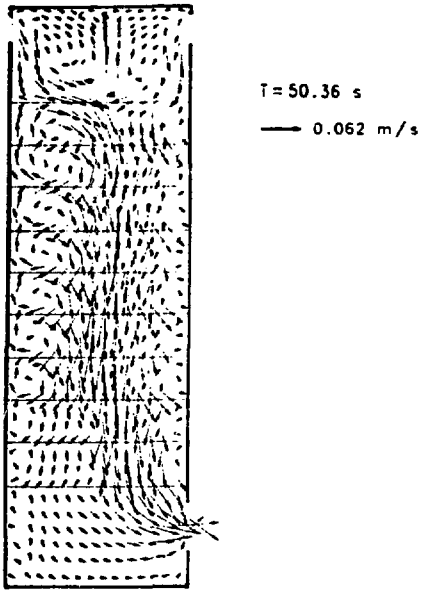

Fig. 5 Transient Flow Pattern at t = 50.36 s.

transient, the flow patterns and temperature maps suggest that the cold fluid entering the upper regions of the heat-exchanger begins to penetrate and channel down through the warm fluid below. A series of vortex rings is also generated between adjacent baffle plates. The size of the vortex rings nearly reach its maximum when the temperature gradient across the tube bundle between the baffles becomes maximum (about 12°C). The radius of the cross section of the toroid-like vortex ring is not uniform. In general, the vortices formed in such a way will move downward, meanwhile, the radii of the rings will increase. However, due to the existence of the baffles, the vortex rings are formed and confined between them.

The radii of the rings are also restrained. According to the vortex theory, the vortices adhere to the fluid; that is, the fluid particles are trapped between the baffles in the "recirculation zone." The energy in the fluid is then dissipated by the fast-moving fluid through the core of the vortices. Such an effect is referred to as "channeling." The transient effect propagates from the distribution shroud toward the outlet pipe. When the thermal-downramp transient input at the flow distribution shroud has been completed, the transient effect in the tube bundle begins to fade. The temperature gradient across the heat-exchanger starts to diminish. The viscous diffusion effect overcomes the generating rate of the vortices. The size and strength of the vortices cease growing and start to shrink.

Finally, the flow pattern returns to the initial steady state configuration under a new equilibrium temperature field. Note also that during the transient, the baffles lose their function as a flow regulator. The baffles under conditions of strong thermal buoyancy are unable to maintain crossflow as they do under the steady-state condition.

One significant finding of this work is that the COMMIX code can predict under conditions of mixed convection, the flow channeling on the shell of an IHX and yield good information on thermal distribution. The calculation also demonstrates that the flow transport time through the heat-exchanger (the time period from the moment the thermal disturbance begins to pass a reference location of the heat-exchanger unit to the moment it reaches the outlet of the unit) can be correctly calculated. The transport time was shown by experiment to be shorter than what would be predicted by 1-D models. The discrepancy is attributed to the fact that the 1-D model lacks the ability to predict the channeling effect (a three-dimensional phenomenon), which causes the thermal disturbance to travel faster through the bundle. The numerical result indicates that such an experimentally observed phenomenon can be duly predicted through a three-dimensional modeling. The flow transit time between shell-inlet pipe to outlet pipe is 71.4 s for test case TX1410 (or ~47.4 s from the inlet flow-distribution shroud to the outlet pipe).[3] The 1-D prediction gives 101.0 s (or ~77.0 s from the inlet flow-distribution shroud to the outlet pipe).[3] The current numerical result gives 47.0 s for the flow transit time (from the inlet flow distribution shroud to the outlet pipe) which is in good agreement with experiment. The error of the one-dimensional prediction is over 40%.

Under steady-state conditions before the thermal transient takes place, the temperature gradient across the heat-exchanger unit at an axial location about three-quarters of the distance through the tube bundle is less than 2°C. However, during the time in which the disturbance passes through the axial location and flow channeling is occuring, the radial temperature variation increased to 12°C. Such temperature gradients (2°C at steady-state and

12°C at transient) have also been observed in the numerical result. The computed and measured temperature at various locations during the transient are shown in Fig. 6-7. The agreement is encouraging.

However, it has also been noticed that the numerical result does not render an accurate prediction at the region that is near or below the shell outlet. It has been found[3] that a rather cool region exists there and contributes

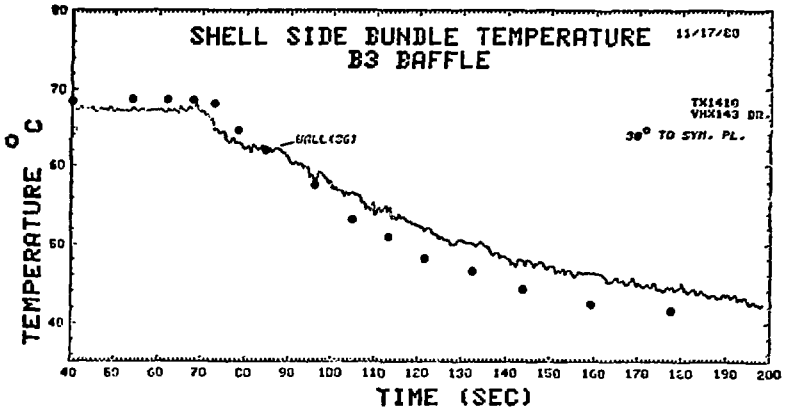

Fig. 6 Comparison of Transient Temperature at Shell-Side Bundle above Baffle B3 near wall.

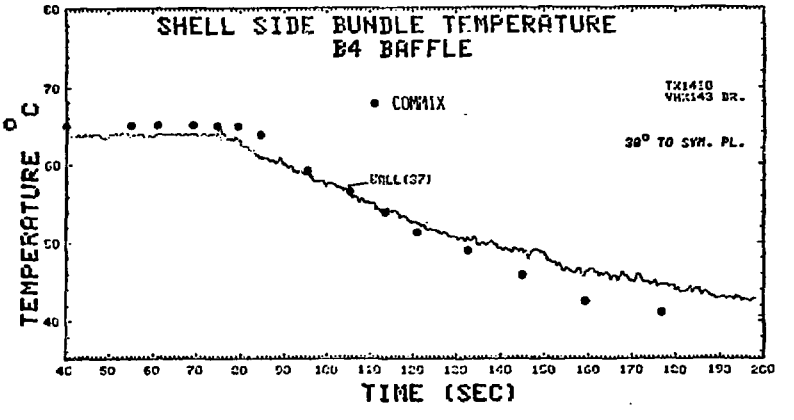

Fig. 7 Comparison of Transient Temperature at Shell-Side Bundle below Baffle B4 near wall.

to a large temperature differential at the outlet pipe and stratification. The heat-transfer mechanism near this region is not well understood and not properly modeled. Further improvement is needed.

The pressure drop between the shell inlet and the shell outlet (see Fig. 1) was also recorded for the TX1410 test case. The reference datum for pressure-gage calibration is equivalent to a hydrostatic pressure shift between the inlet and outlet. Using the same calibration factor, COMMIX-IHX produces a pressure drop which is in good agreement with the test case. Keep in mind that the friction loss between the shell inlet and the flow-distribution shroud is not modeled in this analysis. The comparison is shown in Fig. 8. Overall, the posttest analysis performed with COMMIX-IHX shows the capability and reliability of a three-dimensional transient code in analyzing a complex problem.

References

[1] K. E. Kasza, M. M. Chen, and M. J. Binder, "Initial Considerations on the Influence of Thermal Buoyancy on Heat Exchanger Performance," ASME, 79-WA/NE-3, December 1979.

[2] W. T. Sha, et al. "Three-Dimensional Numerical Modeling of Heat Exchanger," ASME paper 82-NE-1.

[3] K. E. Kasza, et al, "Overview of Thermal-Transient-Induced Buoyancy Phenomena in Pipe and Heat-Exchanger Flows," Paper No. 4, 74th Annual Meeting of the AIChE, Advances In Natural Convection, November 1981.

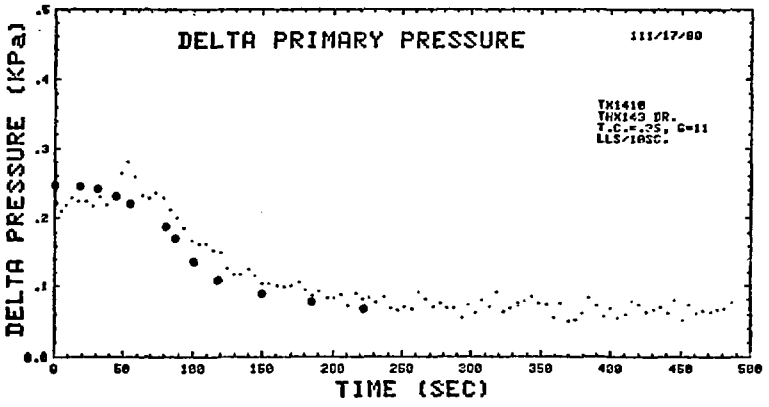

Fig. 8 Comparison of Shell-Side Pressure Drop Data during Transient.

DISCLAIMER